Engineering Structures 48 (2013) 623–634

Contents lists available at SciVerse ScienceDirect

Engineering Structures

journal homepage: www.elsevier.com/locate/engstruct

Behaviors of segmental concrete box beams with internal tendons and external tendons under bending

Aimin Yuan [a,*], Hangs Dai [b], Dasong Sun [c], Junjun Cai [a,b,c]

[a] College of Civil and Transportation Engineering, Hohai University, Nanjing 210098, PR China
[b] College of Civil Engineering, Southwest University, Nanjing 210096, PR China
[c] Jiangsu Provincial Communication Planning and Design Institute Co., Ltd., Nanjing 210005, PR China

ARTICLE INFO

Article history:
Received 18 December 2011
Revised 2 September 2012
Accepted 3 September 2012
Available online 16 January 2013

Keywords:
Segmental prestressed concrete beam (SPCB)
External tendons and internal tendons
Failures modes
Joint opening
Bending

ABSTRACT

Precast segmental prestressed concrete box beam bridges have become the preferred construction method for many elevated highway projects in recent years. These beams, which have internal and external tendons, are increasingly popular because the internal tendons can improve the ductility of the beam, and the external tendons are convenient for maintenance. This study experimentally investigates the behaviors of segmental concrete box beams with hybrid tendons. Three scaled specimens with different ratios of the number of internal tendons to the number of external tendons were tested in detail. The experimental results showed that the ratio had a significant effect on the load-carrying capacity, ductility and failure mode of the beams. The opening of gaps between the segments could not be avoided, and the joint nearest to the applied load was determined to be the critical joint. The assumption that a plane section remained planar under bending was suitable for a crack joint produced by the load. The stress increment rule of the external tendons and internal tendons, as well as the variation of the plain bar strain, were determined.

1. Introduction

Over the past four decades, segmental bridges have been built widely all over the world, especially in the United States, France, Spain, Italy, and China, but most of these bridges are restricted to the use of external or internal prestressing [1,2]. For these bridges, the internal tendons were fully bonded, and the external prestressing tendons were un-bonded. Many problems with segmentally constructed bridges were found as a result of poor construction practices and design errors [3]. In recent year, growing attention has been given to the investigation, development and application of the hybrid tendons systems for the segmental bridge.

Many test investigations on segmental structures have been carried out in several countries over the last few decades. Algorafi et al. [4] presented an experimental investigation of the structural behaviors of externally prestressed segmental (EPS) bridge beams under combined stresses. The studied factors included two different external tendon layouts, two types of joints between segments and different levels of torsional force applied at different load eccentricities. It was concluded that the application of torsion reduced the vertical load and vertical deflection at the onset point of nonlinearity and at a failure load. Torsion not only altered the failure load, tendon strain and beam deflection values but it also altered the failure mechanism. Aparicio et al. [5] presented the results of a test program on externally prestressed concrete beams. Five monolithic and three segmental beams were tested under bending and combined bending and shear. The most significant results were presented, such as the carrying capacity, prestressing steel stress increase at ultimate, and shear behavior of the open joints. It was concluded that the tendon length, as well as the shear behavior of the open joints, has a significant influence on the ultimate load capacity of an externally prestressed beam.

Different FEM models were employed in attempts to reproduce the behavior of the beams, such as joint cracking, opening and failure. Huang and Liu [6] presented an analytical model to investigate the behavior of a prestressed segmental bridge with unbonded tendons under combined torsion, bending, and shear loading. It was concluded that the ultimate bending and shear strengths of monolithic and segmental girders were nearly equal. Ramos and Aparicio [7] and Turmo et al. [8,9] developed a finite element method for the ultimate analysis of an externally prestressed bridge, focusing on the response under combined shear and flexure in service and at the ultimate limit state.

Studies on the relative shear transfer across the joints of adjacent box segments were performed. The effect of the type of joint and epoxy used were examined. The results showed that

* Corresponding author.
E-mail address: zhouyuanhua11@sina.com (A. Yuan).

0141-0296/$ - see front matter © 2012 Elsevier Ltd. All rights reserved.
http://dx.doi.org/10.1016/j.engstruct.2012.09.005

the application of an epoxy-bonding agent provided better assurance of the durability and ultimate shear capacity performance of the joint [10,11]. Turmo et al. [12] presented a test study on the behavior of segmental bridges, focusing on the response of dry castellated joints under shear. Steel fiber reinforced concrete tests were performed on panels with different levels of prestressing, and the shear strengths of dry concrete joints with and without steel fibers were determined. Mohsen et al. [13] and Acrockiasamy et al. [14] carried out a series of tests, including an examination of the shear capacity of epoxy jointed single keys and tests of the fatigue and water tightness at a segment joint. Finite element analysis was also used to model the behavior of the joint specimens. It was observed that all of the shear key specimens failed by fracturing of the concrete along the joint with the shearing of the key. It was observed that epoxy jointing of the specimens enabled the section to attain its monolithic shear strength capacity. The change in the geometry of the shear key caused strain localization along the shear key base, leading to the formation of multiple cracks. Under fatigue loading, the system maintained excellent structural integrity, even after 6 million cycles of load. The deflection measured during the test indicated that no loss of posttensioning occurred as a result of fatigue. It was recommended that AASHTO should be modified to consider the effect of the epoxy. For the same concrete strength, there was an increase of approximately 28% in the shear strength capacity for the hot-weather epoxy specimen in comparison to the cold-weather epoxy specimens. Kaneko and Mihashi [15] performed an analytical study with the objective of developing a model to describe the transition behavior between large single curvilinear cracks and diagonal multiple cracks in shear key joints. The study determined that the cracking transition is induced by a change of the boundary condition. Rombach [16] estimated the ultimate shear capacity of dry joints based on nonlinear finite element analysis. The numerical investigations of the 'bowing' effect showed a significant redistribution of the stresses in the top slab of the bridge.

However, the internal tendons inevitability encounter problems, such as anchor corrosion, poor resistance to the repeated application of tension, difficult replacement, and difficulty in predicting the magnitude of the prestressing force. External tendons also encounter the problem that the prestressing force disappears suddenly if the deviator or anchor block breaks down. None of the previous studies has examined prestressed segmental concrete box beams with both external and internal tendons. Recently, the Sutong Yangtze River bridge and the Nanjing No. 4 Yangtze River bridge in China were built using such hybrid tendons. The construction of such novel prestressed segmental concrete box beams offers some advantages, such as the following:

(1) Reduction of the duration of construction at the site and shortening of construction periods. The construction of the segmental concrete bridges with both external tendons and internal tendons can speed up when it is associated with a span-by-span construction process. For the construction of each of the spans, the concrete segments are placed next to each other, suspended from a beam or arranged in a mobile falsework, and assembled by means of external prestressing and internal prestressing.
(2) Improvement of the durability and quality of the structure by factory production of segmental beams and the ability to replace the external tendons over time and apply epoxy resin between the joint faces of the segments.
(3) Improvement of the ductility by use of internal tendons. The more significant characteristic of this beam construction is the nonexistence of bond reinforcement crossing the joint faces. Therefore, the addition of internal tendons will inevitably improve the beam ductility because of the bonding force.

The principal goal of this study highlights the behaviors of segmental concrete beams with both external and internal tendons. As far as the authors are aware, this is the first time that the response of a segmental box beam to the use of a hybrid tendon configuration has been studied. The effect of the ratio of external tendon number to internal tendon number was considered to be an important factor. The test results, including the load–deflection curves, failure modes, stress variations of the tendon and plain bar, are also given to provide a better understanding of the behavior of the segmental concrete box beam with hybrid tendons.

2. Test specimens

To investigate the effect of hybrid tendons, three prestressed segmental concrete box beams were precast using the long-line match casting method. The details of the beams are shown in Fig. 1. It was assumed that the bridge box beam would be constructed in the Nanjing No. 4 Yangtze River bridge. The scaling factor of the specimen was one-tenth. Each beam consists of 12 segments, and there were five types of segments, indicated by letters from A to E. The dimensional details of a half section of the box beam are shown in Fig. 2. It was observed that the thickness of the bottom slab changed at the C segment from 12 cm to 10 cm, and the thickness of the web changed at the D segment from 10 cm to 8 cm. The specimens had a height of 60 cm from the upper surface of the top slab to the downward surface of the bottom slab, and they also had a width of 150 cm at the top flange.

Three segmental box beams were produced separately. Epoxy resin was spread on the joint surface. After all segments were assembled, a prestressing force was applied to ensure that the epoxy resin could spread uniformly. The commercially available epoxy consists of a mixture of two resins that are combined at specified proportions to achieve the finial bonding material. A very thin layer of epoxy, approximately 1 mm on each side, was applied to the surfaces of both the male and female joint area. Then, the high strength mortar was grouted into the sheath after the internal tendons were inserted into the sheath and tensioned.

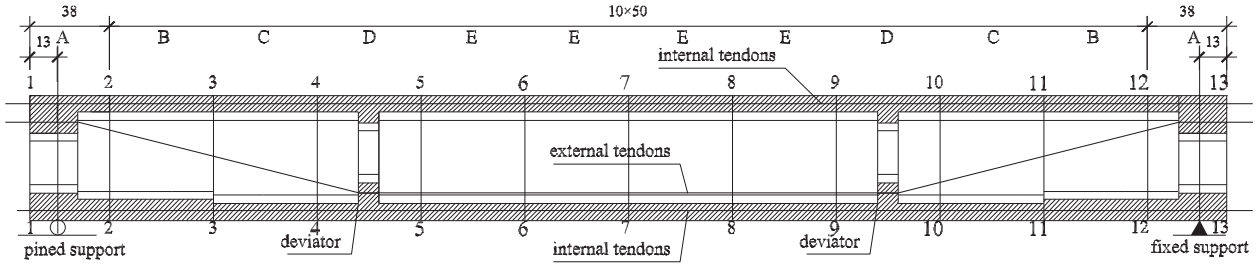

Fig. 1. Divided segment components (units: cm).

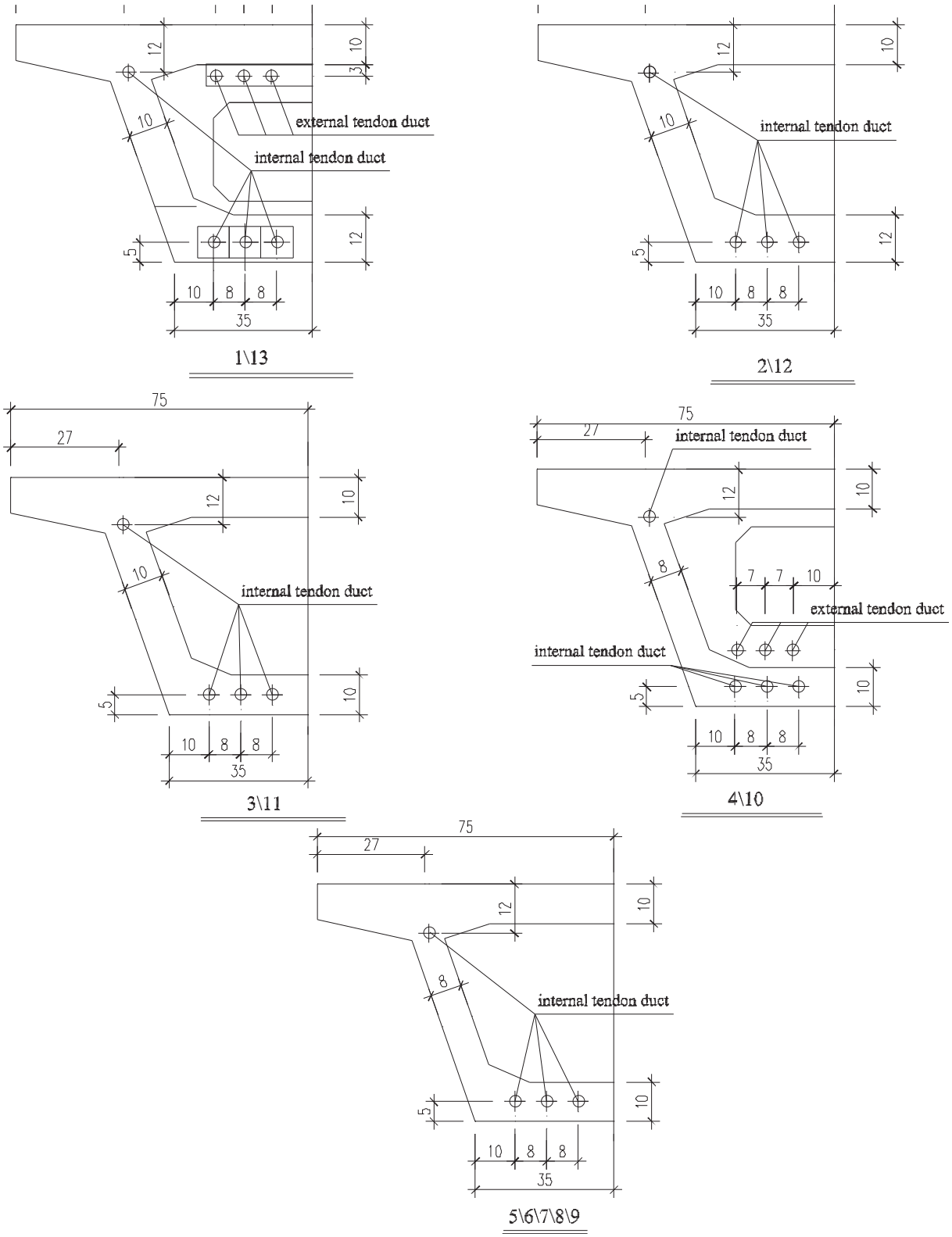

Fig. 2. Specimen dimensions and tendon allowance ducts (units: cm).

There were six allowance ducts inside of the box beam for the internal tendons, six allowance ducts at the end of the beam, and a deviator for the external tendons. Another two ducts were set aside for the constructional tendons. The additional internal tendons were placed in the top floor to ensure that no cracking occurred with the application of the prestressing force. For the three segmental beams, the ratios of constructional tendons to internal tendons to external tendons were 2:6:2, 2:4:4, and 2:2:6. For convenience, the three segmental prestressed concrete beams (SPCBs) are called SPCB2-6-2, SPCB2-4-4 and SPCB2-2-6, respectively. The per bonded internal tendons consisted of seven wires of Φ5 mm (the area of each tendon was 98.7 mm^2) per

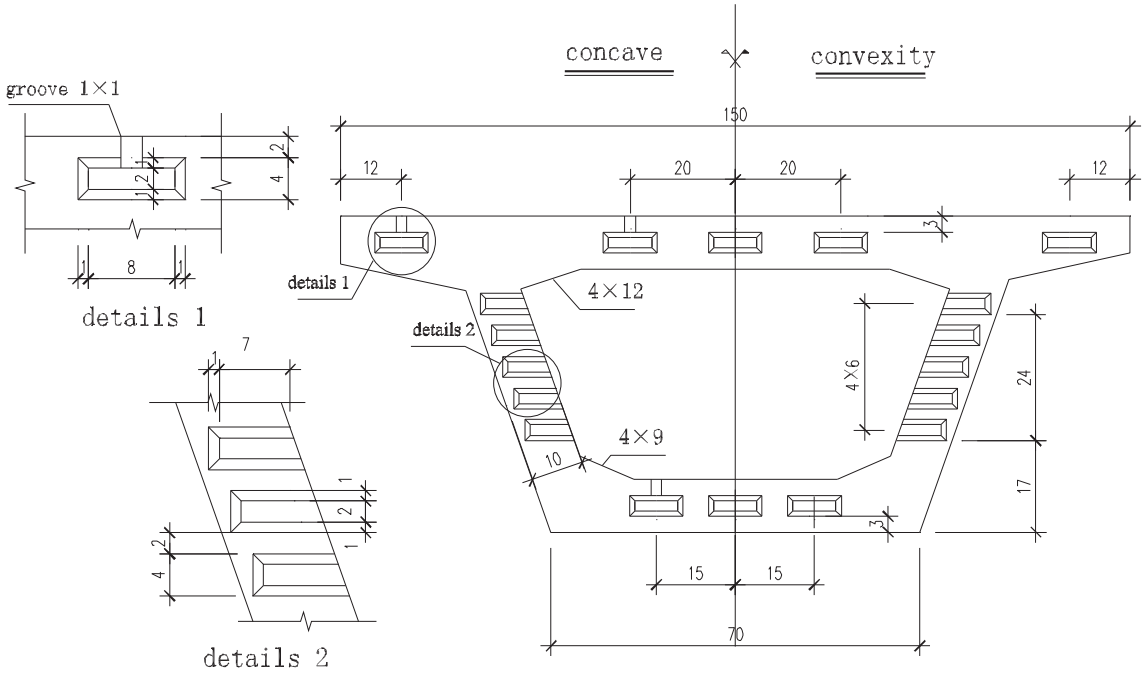

Fig. 3. Shear key joint type: concave (left), convex (right) (units: cm).

Table 1
Property of materials.

Concrete type	Compressive strength (MPa)	Concrete modulus of elasticity (MPa)	Density (kN/m^3)
Silicate cement concrete	32.2	2.37×10^4	25.0

strand. Unbonded external prestressed tendons were used, which were only in contact with the beam at the anchorages and deviator. The external tendons, similarly to the internal tendons, contained seven wires of Φ5 mm (the area of each tendon was 98.7 mm^2) per strand, except that the external tendons were enclosed in a PE sheath.

To ensure a uniform distribution of the prestressed forces on the beam and local load bearing capacity, eight thick steel plates (100 mm × 100 mm × 12 mm) and one thick steel plate (550 mm × 100 mm × 12 mm) were placed at the end of the beam.

The exact dimensions of the keys, such as the shear key depth and center-to-center distance on each side of the joint, are shown as Fig. 3. The male–female shear key had the same scaled dimensions as those in the actual design of the precast concrete segment. The trapezoidal shape of the key had a 10 cm × 4 cm base area and an 8 cm × 2 cm top area with a 1 cm depth.

Depending on the type of mix, the properties of the aggregate, and the time and quality of curing, commercially produced concrete can be prepared with compressive strengths up to C40. Table 1 shows the properties of the concrete used in the test. The compressive strength is a mean value obtained from three cubic specimens with standard deviation 3.1 MPa.

Because of the high creep and shrinkage losses in concrete, effective prestressing can be achieved with very high-strength steels, in the range of 1860 MPa or higher. Such high-stressed steels are able to counterbalance these losses in the surrounding concrete, and they have adequate leftover stress levels to sustain the required prestressing force. Table 2 shows the strengths and geometrical properties of the bonded tendons and unbonded tendons with seven wires.

The fabrication of the precast hollow box girder specimens is summarized in Fig. 4.

3. Test setup and instrumentation

The assembly of the beam was carried out by arranging the segments close together on a temporary parallel steel tube. The external prestressed tendons were laid through the anchors and deviators, and the internal prestressed tendons were also placed by the anchors.

The beam was tested with two concentrated loads applied to the 1/3 span location. A four-point load with a 1834 mm length and 700 mm width was applied using a jack with a capacity of 1000 kN. The magnitude of the load was recorded by the load cell. The prestressed load was applied using a jack with a capacity of 300 kN at each tendon. The prestressing force was also measured by the load cell sensor.

The supporting arrangement at the bottom of the beam was designed to simulate a hinge support with two solid steel shafts with diameters of 50 mm. At one end, the beam was fixed against axial and vertical deformation, and only rotation was allowed. At the

Table 2
Seven wire standard strand for prestressed concrete.

Types of reinforcement	Nominal diameter of strand (mm)	Breaking strength of strand (f_{ptk}) (MPa)	Nominal strand area (mm^2)	Friction coefficients	Weight per meter (kN/m)
Bonded	$1 \times 7 - \phi 12.7$	1860	98.7	/	0.84
Unbonded	$1 \times 7 - \phi 12.7$	1860	98.7	0.004	0.84

(1) Wood mold

(2) Steel binding

(3) Casting of odd numbered segments

(4) Casting of even numbered segments

(5) Tendon placement

(6) Spreading of epoxy resin

(7) Duct grouting

Fig. 4. Fabrication procedure.

(a) Test setup

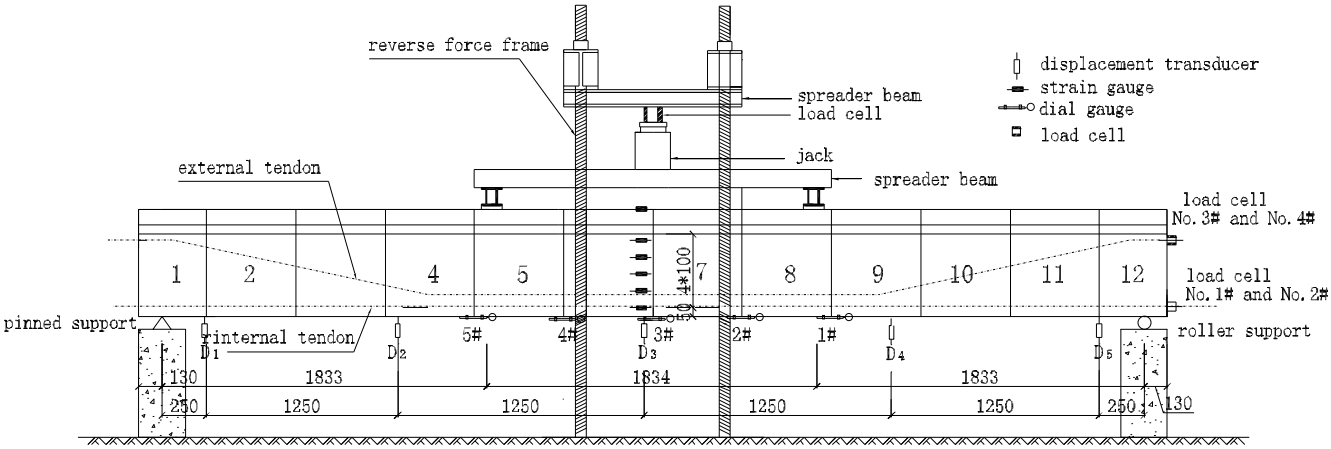

(b) Instrumentation layout

Fig. 5. Test setup and instrumentation layout.

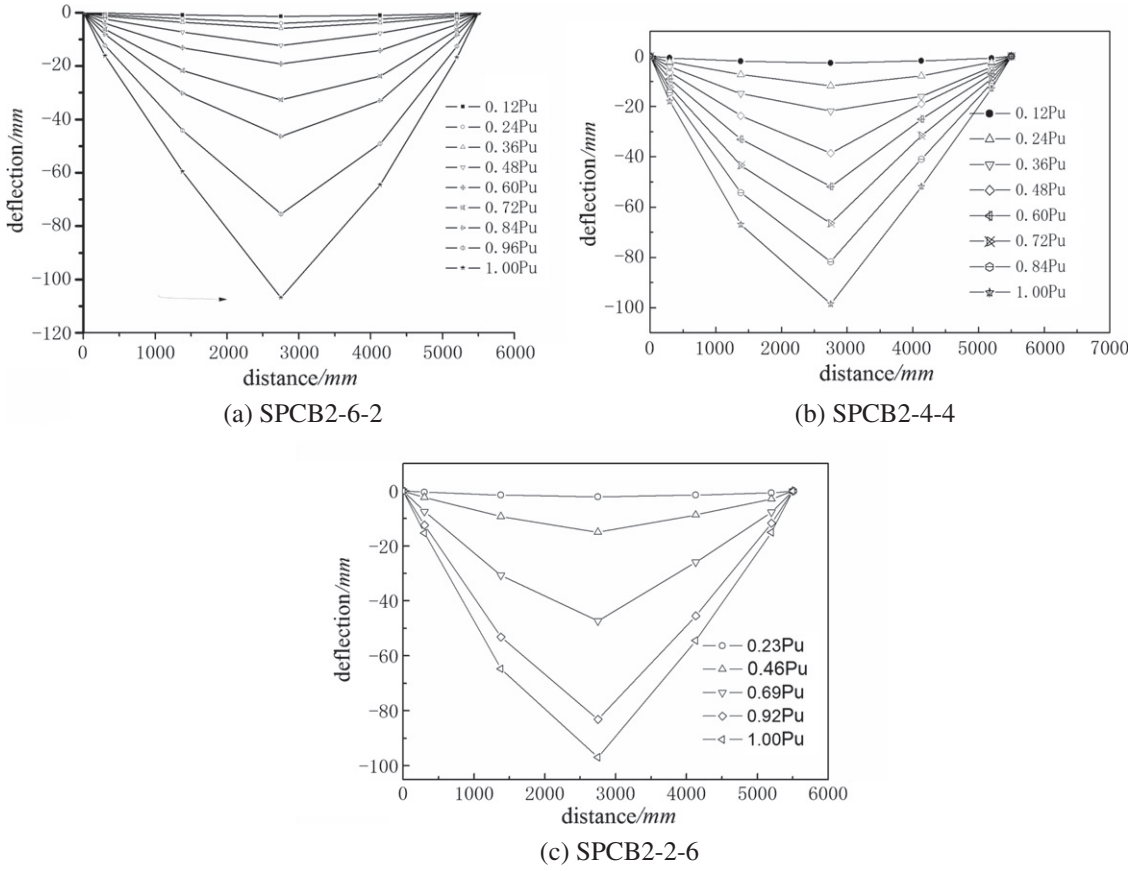

(a) SPCB2-6-2

(b) SPCB2-4-4

(c) SPCB2-2-6

Fig. 6. Deformation of each segmental prestressed concrete beam.

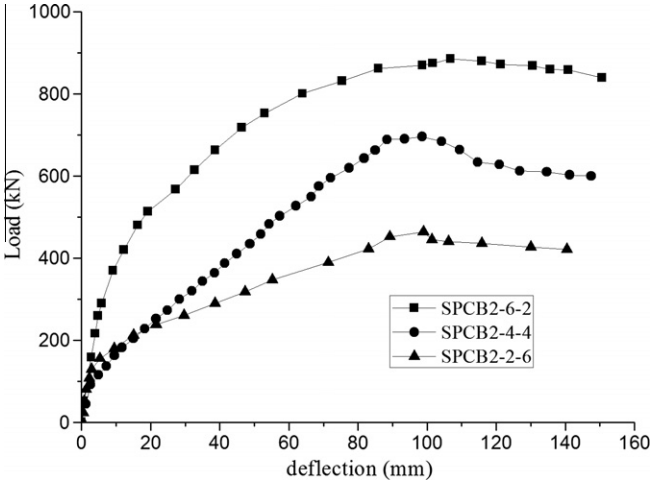

Fig. 7. Relationship between the deflection and the vertical load.

other end of the beam was a roller support that allowed both axial and rotational deformation.

Vertical deformation was measured using a displacement transducer located at the $L/2$ span, the $L/4$ span and the support. Mechanical dial gauges were placed at different locations on the crack joints. Strain gauges were placed at the top and side surfaces of the No. 6 segment. The entire test setup and instrumentation distribution are shown in Fig. 5.

Before the test began, the external tendons and the internal tendons were tensioned. The limitations of the control prestressing for the external tendons and the internal tendons were $0.65f_{ptk}$ and $0.75f_{ptk}$, respectively.

Table 3
Ductility indices of all tested beam.

	SPCB2-6-2	SPCB2-4-4	SPCB2-2-6
Deflection ductility ($\mu\Delta$)	2.9017	1.8136	1.8966
Energy ductility (μ_E)	4.0816	2.3923	2.4012

4. Test results

4.1. Deformation characteristics

The vertical load was applied gradually until failure. Before the load reached its maximum value, the force control method was adopted. When the beam reached its maximum load-carrying capacity, the displacement control method was adopted.

Fig. 6a–c shows the distribution of the deflection along the segmental box beam length for each beam at different values of the vertical load. As the vertical load increased, the vertical displacement of the beam also increased gradually, behaving as a monolithic beam. No relative vertical displacement between the segments was observed at any point during the test.

Fig. 7 shows the load–vertical deflection curves at the mid span for all types of hollow box girder. The relationship was initially linear, and the response became nonlinear until failure with further increase of the applied load. In addition, it was observed that at any value of the vertical load, the deflection of the beam increased with increasing load. Consequently, the stiffness of the beam

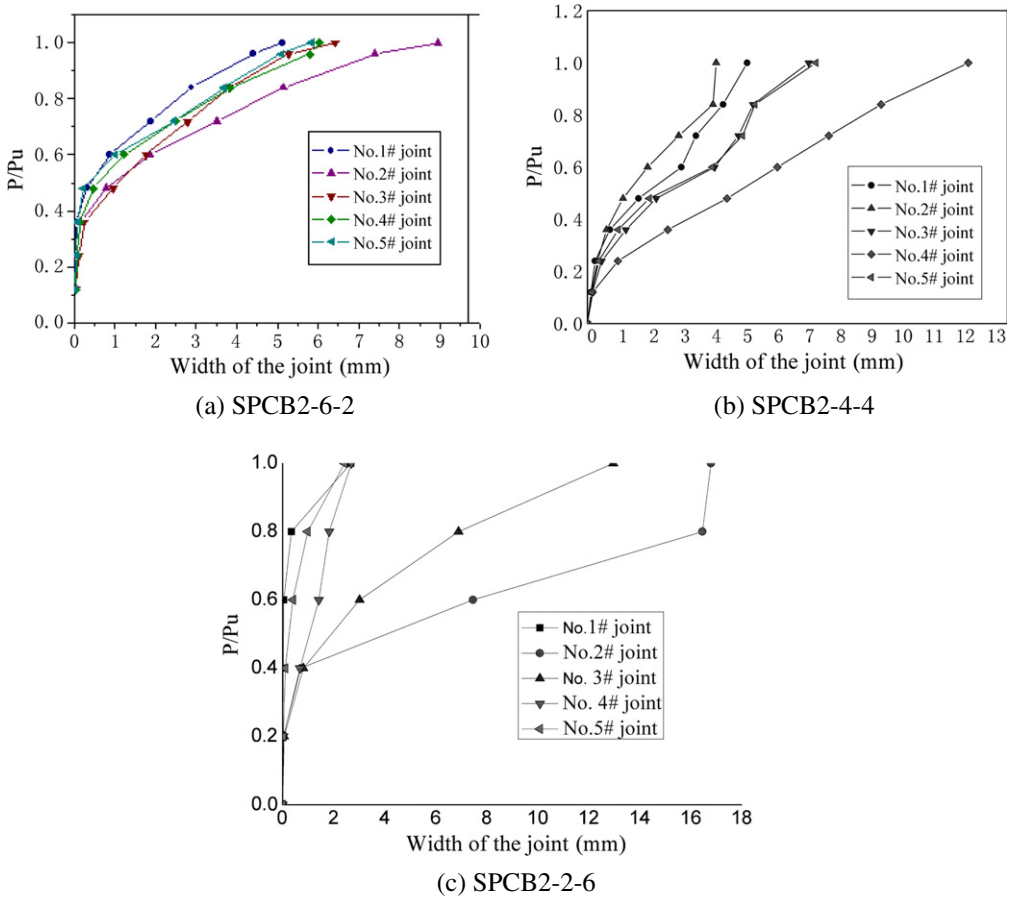

Fig. 8. Width of the joint opening for each beam segment.

decreased as the load increased because of the joint crack, the non-linear behavior of concrete in compression, yielding of the steel and geometrical non-linear behavior.

In the case of the SPCB2-6-2, SPCB2-4-4 and SPCB2-2-6 beams, the relationship was linear up to vertical loads of 200 kN, 130 kN and 90 kN, respectively. After those values, the response was non-linear up to 880 kN, 690 kN and 480 kN, respectively. This result also indicates that the ratio of the internal tendon number to the external tendon number had a significant effect on the load bearing capacity of the beam. Greater numbers of internal tendons resulted in higher achieved load bearing capacity of the beam.

To reflect the physical characteristics of the beam, the following definitions of structural ductility are adopted.

- Deflection ductility: $\mu_\Delta = \Delta_u/\Delta_y$.
- Energy ductility: $\mu_E = E_{tot}/E_y$,

where Δ_u = midspan deflection at ultimate failure; Δ_y = midspan deflection at yielding of tension steel; E_{tot} = area under the load-defection curve at ultimate failure (total energy); and E_y = area under the load–deflection curve at yielding of tension steel.

However, with hybrid tendons segmental beams, there is no yield point. The definitions of equivalent yield point proposed by Park are adopted in present study. The yield deflection Δ_y is taken as the deflection at the hypothetical yield point of an equivalent perfectly elasto-plastic system with an elastic stiffness equal to the secant stiffness of the section at 75% of the peak resisting load and a yield load equal to the peak resisting load itself. The ductility indices were calculated for all the three beams tested in this study, and these are summarized in Table 3. From this table, it is evident that the beam with higher hybrid ratio failed in a more ductile manner than did the other two beams with lower hybrid ratio. The use of the internal tendons increased both the deflection ratio and energy ratio. Therefore, we recommend that the ratio of this hybrid tendons should not be less than 1:1.

4.2. Width of the open cracks near joints

From Fig. 8, it was observed that the segment joint remained closed with applied loads as high as $0.2P_u$. At such a low range of applied vertical loads, the segmental prestressed beam behaved as monolithic beam. However, after reaching the decompression bending moment, the opening cracks between the segment near joints increased until failure as the applied load increased. Fig. 8 also shows that the width of the cracks did not increase linearly with increasing load. In particular, the width of one of the cracks was much greater than that of the others. This phenomenon was mainly attributed to the presence of critical cracks near the 2# or 4# joint, where the first joint was located at the pure moment zone and nearest to the applied load location. Fig. 8c shows that the opening crack widths of the 2# and 3# cracks were much larger than the others. This result indicates that there were two plastic hinge emergences during the test because of the deviator failure prior to the crush of the concrete joint.

4.3. Tendon force variation

Figs. 9 and 10 illustrate the variations of stress in the internal tendons and the external tendons with the application of vertical load for all beams. With the increase of the applied load, the

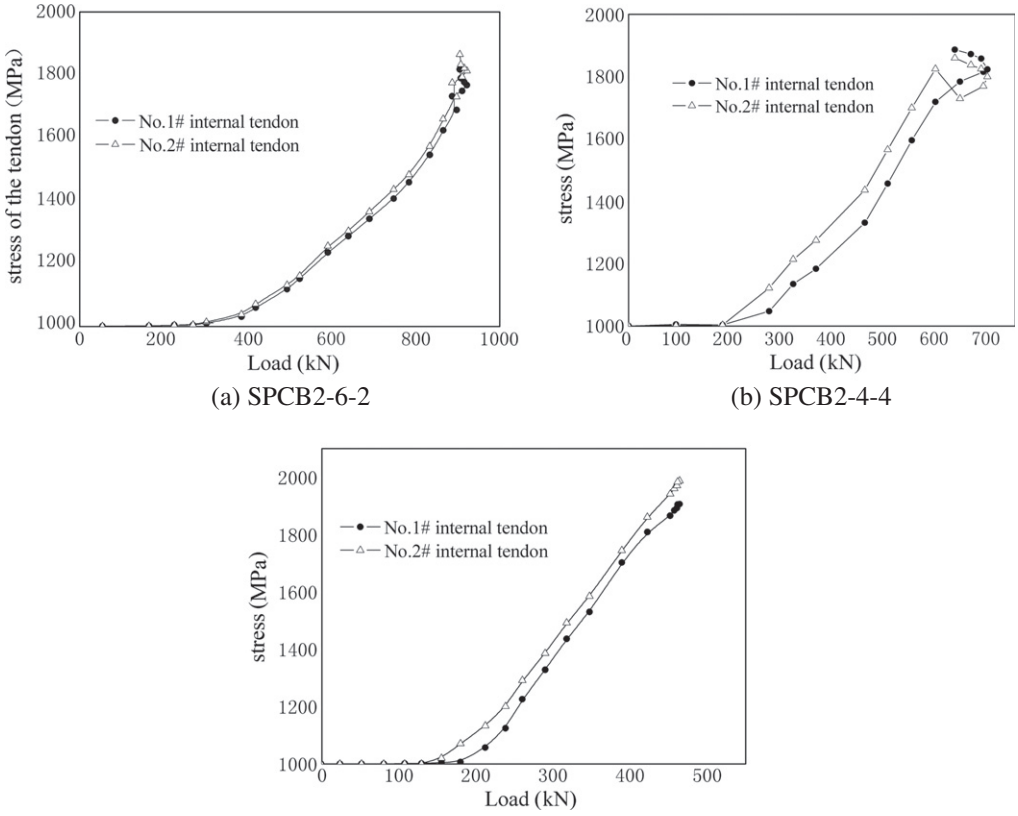

(a) SPCB2-6-2 (b) SPCB2-4-4

(c) SPCB2-2-6

Fig. 9. Load–stress relationship for the internal tendons.

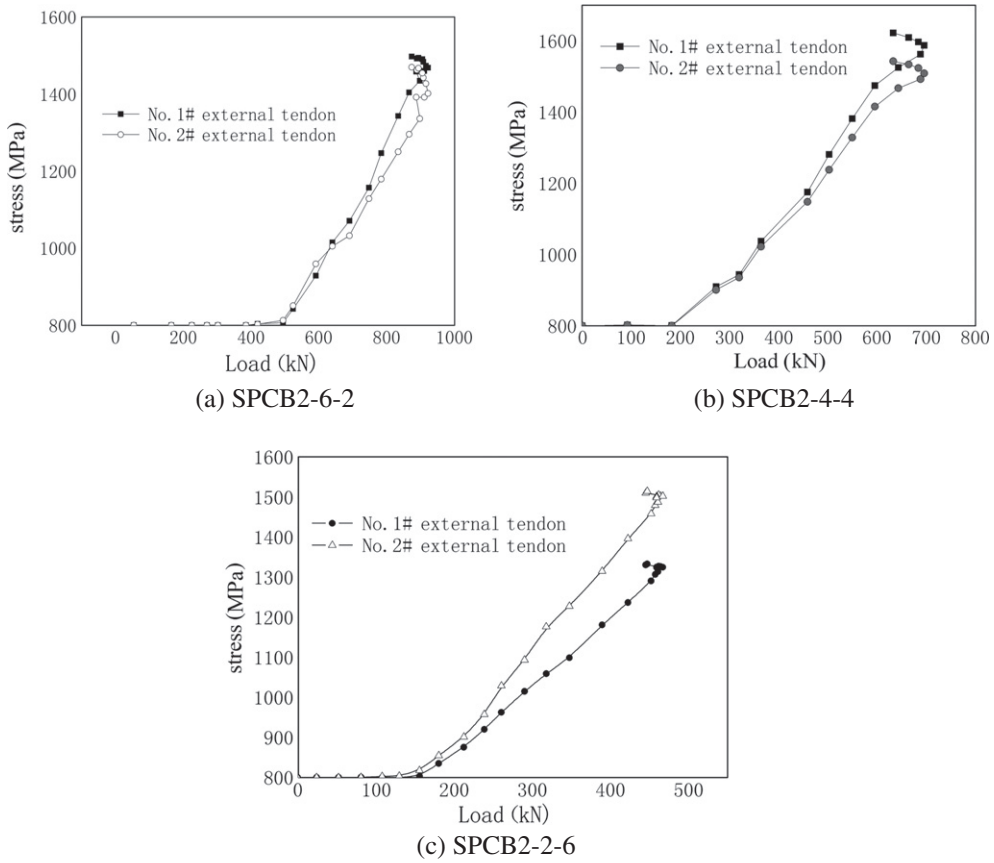

(a) SPCB2-6-2 (b) SPCB2-4-4

(c) SPCB2-2-6

Fig. 10. Load–stress relationship for the external tendons.

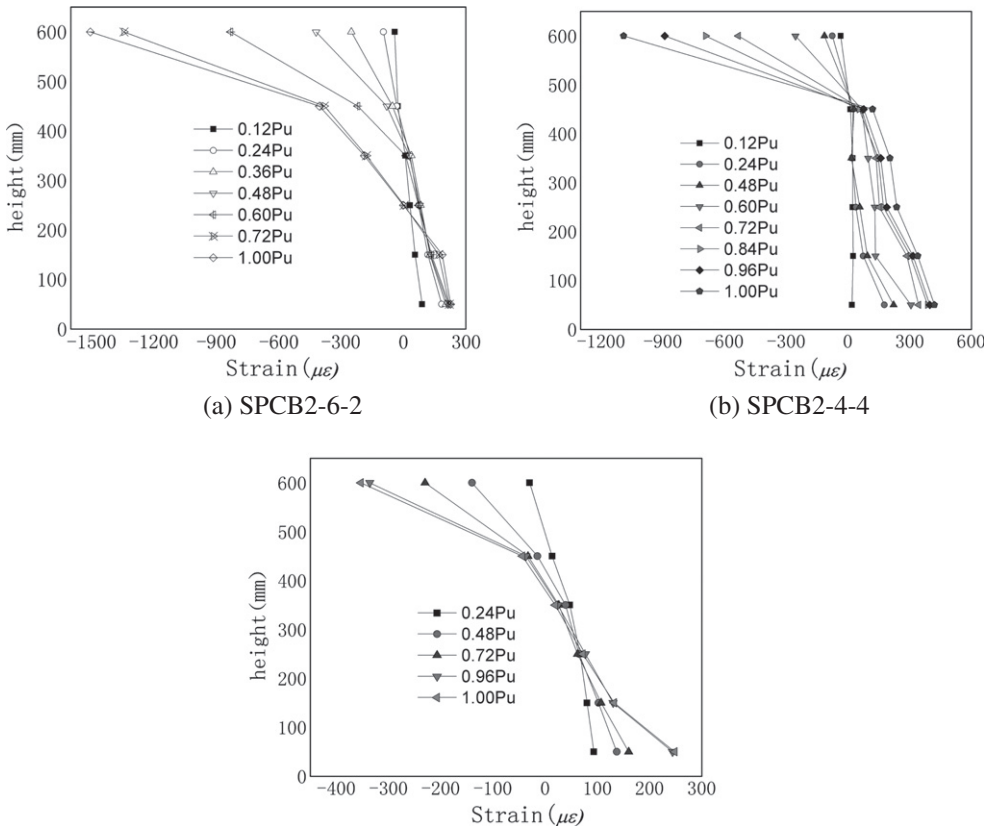

(a) SPCB2-6-2 (b) SPCB2-4-4

(c) SPCB2-2-6

Fig. 11. Strain distribution across the mid-span section at various loading increments.

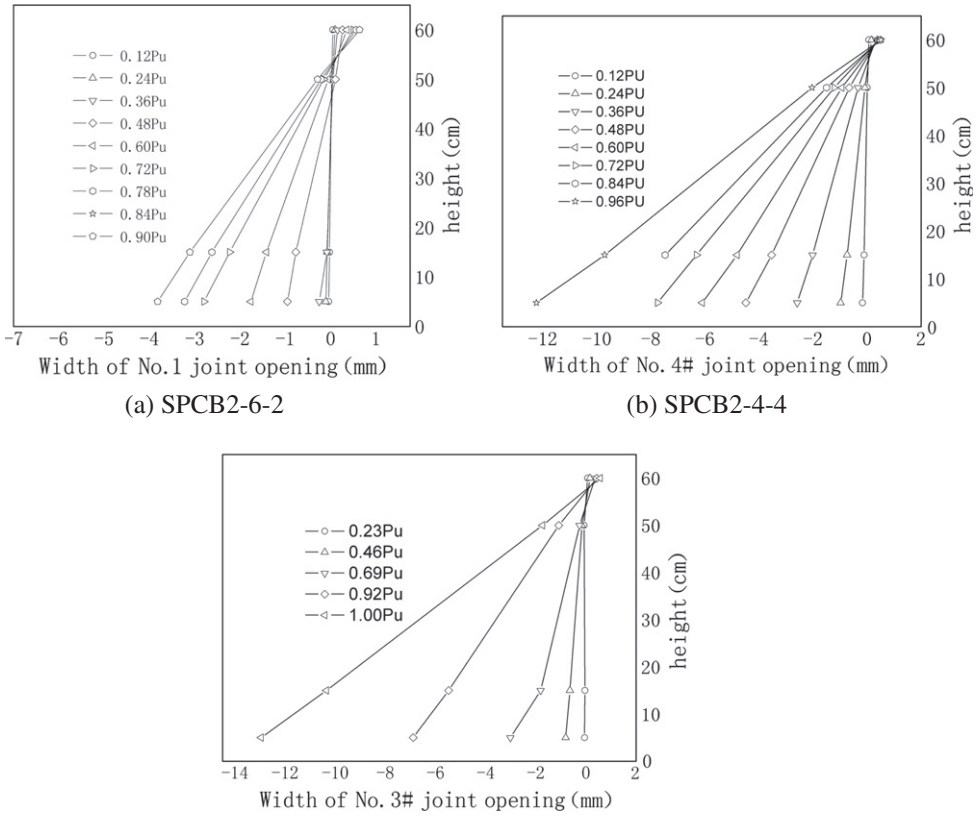

(a) SPCB2-6-2 (b) SPCB2-4-4

(c) SPCB2-2-6

Fig. 12. The width distribution across opening joint section at various loading increments.

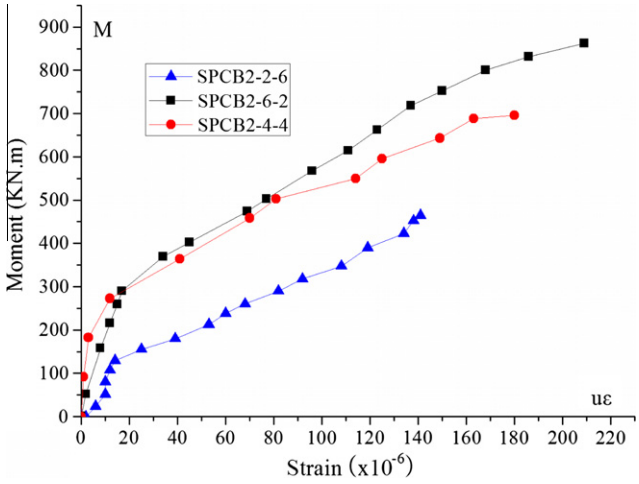

Fig. 13. Strain variation of the plain bar at the bottom slab.

tendon stress remained constant until the cracking load was reached. With a further increase of the applied load, the response increased as a result of the extension of the tendon length. When the beams failed because the concrete was crushed, the strength of the internal tendons reached as high as 1860 MPa, which was the standard tension strength of the tendons. The strength of the external tendons reached approximately 1400 MPa. From these figures, it can also be concluded that the stress increases of the internal tendon and external tendons were approximately 40% and 30%, respectively.

Another well known phenomenon can be observed by comparing Fig. 9 with Fig. 10. From the cracked load to the ultimate load, the incremental stress of the internal tendons was greater than that of the external tendons. This phenomenon certainly attributed to the fact that internal prestressing has strain compatibility with the surrounding concrete and the external prestressing has only displacement compatibility at the points in contact with the concrete, this is to say, at anchorages and deviators. Also external tendons has lower lever arm and the second-order effect. The shift of the tendon eccentricity and possible slippage at the deviation points occurred during the test, especially at the ultimate load stage.

4.4. Concrete strain variation

Fig. 11 shows the longitudinal strain in the concrete at various points across the mid-span section along the height. Because some slippage had occurred between the internal tendon and the surrounding concrete, some deviation from linearity was also observed. Bernoulli's principle was not completely applicable to the concrete in the neighborhood of the crack joints. The assumption that a plane section subjected to bending remained planar after bending did not hold in the regions of the segmental beam without cracks.

However, if the width of the joint opening was measured over a dial gauge length (15 cm) that included one joint crack, Bernoulli's principle was found to apply to this average tensile strain. Fig. 12 shows the width distributions measured across sections of a crack joint at the failure regions with various loading increments. It is evident from Fig. 12 that the measured width profiles were reasonably linear. Certainly, the assumption of plane sections remaining planar was sufficiently accurate for the purpose of design. As the load increased, the compression strain at the top increased at a high rate because of redistribution of stress caused by opening.

4.5. Longitudinal plain bar strain variation

Fig. 13 shows the strain variation of the longitudinal plain bar of the bottom slab at the No. 6 segment for all beams with the moment. The curves clearly consist of two straight lines. From the zero point to the turning point, the strain in the plain bar increased and decreased the compression strain produced by prestressing. At the turning point, the compression strain in the plain bar was reduced to zero. From the turning point to the point of failure, the longitudinal plain bar began to acquire tensile strain as the applied load increased. However, the bar strain was very small and far from

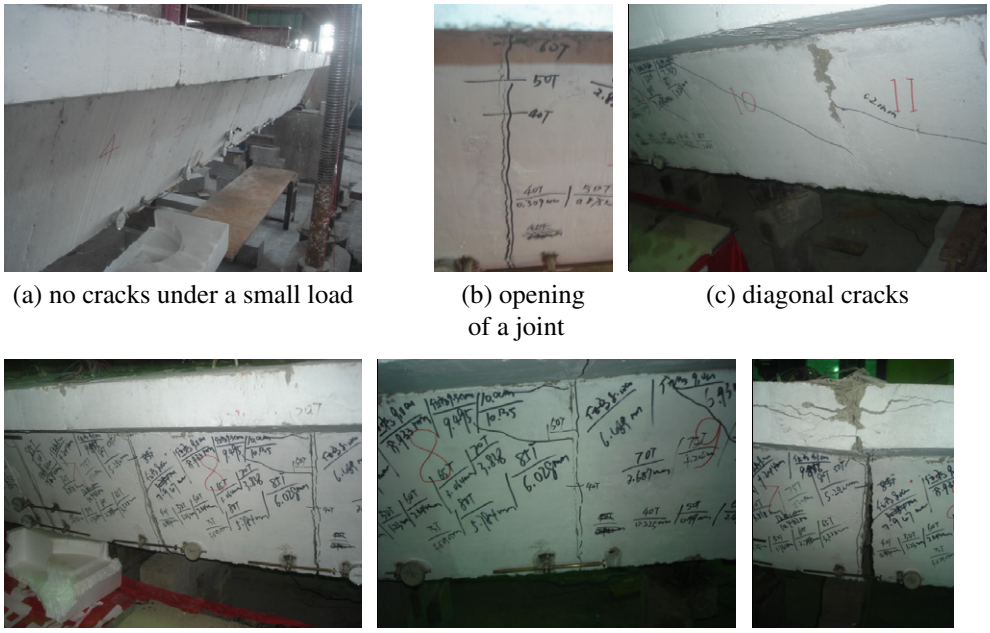

(a) no cracks under a small load

(b) opening of a joint

(c) diagonal cracks

(d) further opening of joints crushing

(e) crack propagation

(f) failure due to concrete

Fig. 14. SPCB2-6-2 box beam failure sequence and failure mode.

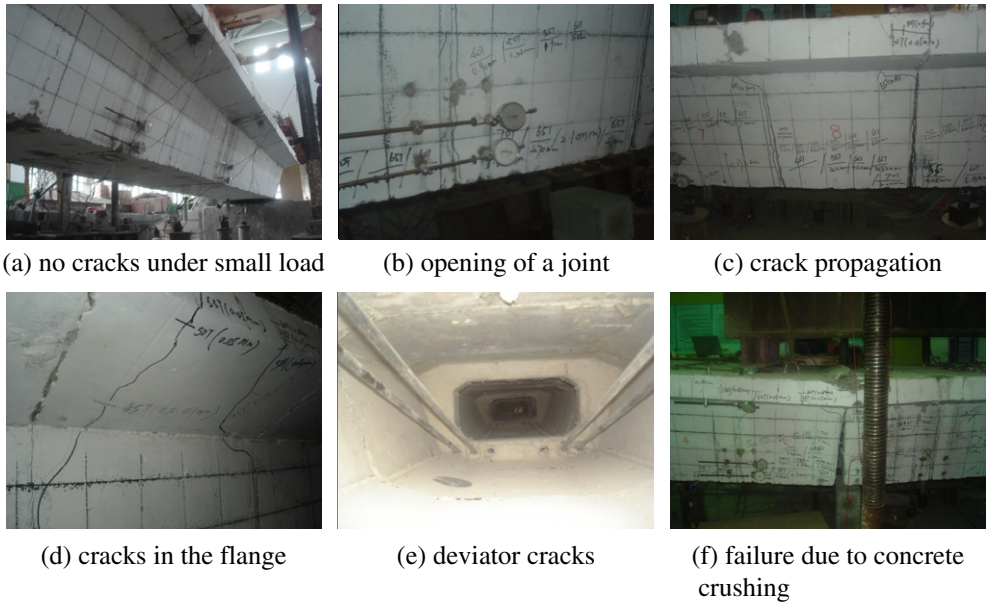

(a) no cracks under small load (b) opening of a joint (c) crack propagation

(d) cracks in the flange (e) deviator cracks (f) failure due to concrete crushing

Fig. 15. SPCB2-4-4 box beam failure sequence and failure mode.

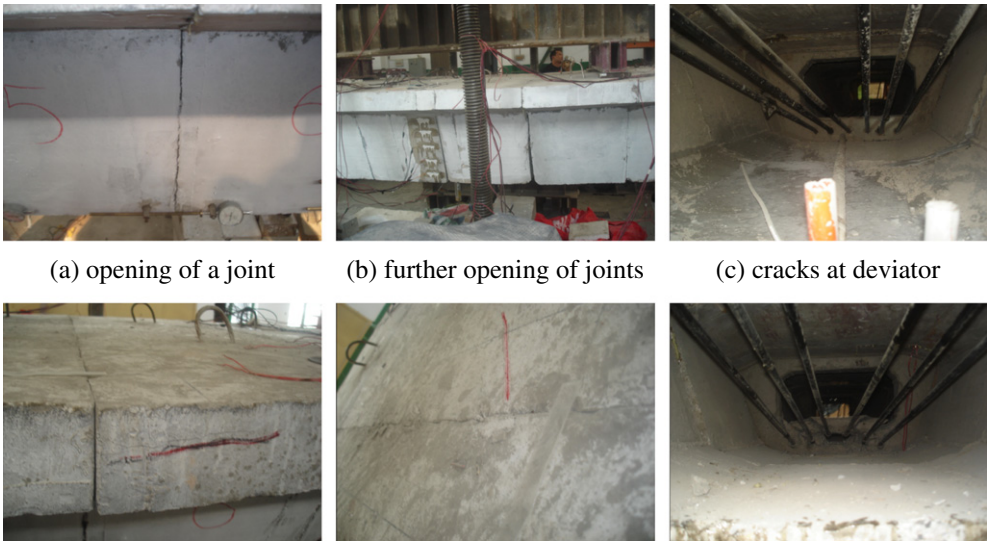

(a) opening of a joint (b) further opening of joints (c) cracks at deviator

(d) crack propagation (e) top surface concrete crushed (f) failure due to deviator

Fig. 16. SPCB2-2-6 box beam failure sequence and failure mode.

the yield strain. The strain remained small because the No. 6 segment was subjected to pure moment action, and no unbalance force was produced.

4.6. Failure mode

Before the opening of the joints occurred, the segmental hybrid prestressed beam worked as an integrity structure. As the load increased, the decompression bending moment was reached. The initial compressive stress produced by the prestressed force was reduced to zero. When the crack load was reached, a critical joint opened. A slight increase in load resulted in further wide cracking. Consequently, the contact area between the segments was reduced, and the compression fiber of the concrete was increased. With this increase in strain, the distribution of the compressive stress in the concrete became distinctly nonlinear. Because the tendon content of the section was right, the tendons reached their yield strength before the concrete reached its maximum capacity. The reduction in the neutral axis depth caused a slight increase in the lever arm. The flexural strength of the joint section was reached when the strain in the extreme compression fiber of the concrete was reached.

Figs. 14–16 show the beam failure sequence. In general, some cracks developed near the joint as the vertical load increased. The failure of SPCB2-6-2 and SPCB2-4-4 occurred suddenly when the top slab concrete was crushed. However, the failure of beam SPCB2-2-6 occurred because of deviator destruction.

Additionally, diagonal cracks only appeared in the web of beam SPCB2-6-2. This result indicates that as more inclined external tendons were used, higher shear resistance was achieved.

5. Conclusions

A series of tests were conducted to study the behaviors of precast segmental box beams with internal and external tendons. Some important conclusions are listed as follows:

(1) As the ratio of the internal tendon number to the external tendon number was varied from 6:2 to 4:4 and 2:6, the test results indicated that the ratio had a significant effect on the load-carrying capacity and ductility of the beam. As more internal tendons were laid out, higher load-carrying capacity and better ductility were achieved. Therefore, the ratio of this hybrid tendons not less than 1:1 was recommended.
(2) It was shown that joint opening was difficult to avoid at the three different prestressing levels. A significant amount of gap opening was observed next the joint at the pure bending zone in each test, and one of the cracks developed a critical crack opening adjacent the joint nearest to the applied load. For a beam with a multi-deviator, if the deviator was destroyed prior to the crushing of the beam concrete, more critical crack opening was observed.
(3) The stress increments of the internal tendons and external tendons were approximately 40% and 30%, respectively. Because the external tendons were laid out inside of the box beam near the neutral axis and had a second-order effect, their stress increment was less than that of the internal tendons.
(4) In the regions where no cracks appeared for the mid-span segment, the assumption that a plane section subjected to bending remained planar after bending did not hold. However, for a crack joint, the measured strain profiles were reasonably linear. The assumption that plane sections remained planar was suitable for the purpose of design.
(5) The variation of the plain bar strain showed that the strain was small and far from the yield strain. Its moment–strain curves consisted of two straight lines. From the zero point to the turning point, the initial compression strain produced by prestressing was released. From the turning point to failure, the plain bar acquired tensile strain, which was caused by the frictional force between the internal tendons and the surrounding concrete. It is recommended that a minimum reinforcement ratio ρ not less than 0.2 could be adopted.
(6) As the bending moment increased, the opening between the joints increased, and small cracks developed near the deviator, as well as in the concrete at the top slab of the middle segment. Two of the three beams failed because the concrete was crushed at the top of the critical joint between the segments. Another beam failure occurred suddenly because the deviator was destroyed. The use of inclined external tendons prevented the appearance of diagonal cracks in the web.

Acknowledgements

This study was funded by the Doctoral Fund of the Ministry of Education of China and the Transportation Science Project of Jiangsu Province (Grant No: 08Y08). The financial support of these organizations is gratefully acknowledged.

References

[1] Below KD, Hall AS, Rangan BV. Theory for concrete beams in torsion and bending. ASCE J Struct Eng 1975;101(8):1645–60.
[2] Misic J, Warwaruk J. Strength of prestressed solid and hollow beams subjected simultaneously to torsion, shear and bending. ACI J 1975;SP55:515–45.
[3] Wouters JP, Kensner K, Poston RW. Tendon corrosion in precast segmental bridges. Transportation research record, 1211. Transportation Research Board, Washington, D.C.; 1999. p. 128–32.
[4] Algorafi MA, Ali AAA, Othman I, Jaafar MS, Anwar MP. Experimental study of externally prestressed segmental beam under torsion. Eng Struct 2010;32:3528–38.
[5] Aparicio AC, Ramos G, Casas JR. Testing of externally prestressed concrete beams. Eng Struct 2002;24(1):73–84.
[6] Huang Z, Liu XL. Modified skew bending model for segmental bridge with unbonded tendons. J Bridge Eng, ASCE 2006;11(1):59–63.
[7] Ramos G, Aparicio AC. Ultimate analysis of monolithic and segmental externally prestressed concrete bridges. J Bridge Eng, ASCE 1996;1(1):10–7.
[8] Turmo J, Ramos G, Aparicio AC. FEM study on the structural behavior of segmental concrete bridges with unbonded prestressing and dry joints: simply supported bridges. Eng Struct 2005;27(11):1652–61.
[9] Turmo J, Ramos G, Aparicio AC. FEM modelling of unbonded post-tensioned segmental beams with dry joints. Eng Struct 2006;28(13):1852–63.
[10] Bishara AG, Papakonstantinou NG. Analysis of cast-in-place concrete segmental cantilever bridges. J Struct Eng, ASCE 1990;116(5):1247–68.
[11] Koseki K. Shear strength of joints in precast segmental bridges. Master's thesis, University of Texas at Austin, Austin, Tex; 1981.
[12] Turmo J, Ramos G, Aparicio AC. Shear strength of dry joints of concrete panels with and without steel fibres: application to precast segmental bridges. Eng Struct 2006;28(1):23–33.
[13] Issa Mohsen A, Abdalla Hiba A. Structural behavior of single key joints in precast concrete segmental bridge. J Bridge Eng, ASCE 2007;12(3):315–24.
[14] Arockiasamy M, Badve P, Rao V, Reddy DV. Fatigue strength of joints in a precast prestressed concrete double tee bridge. PCI J 1991;36(1):84–97.
[15] Kaneko Y, Mihashi H. Analytical study on the crack transition of concrete shear key. Mater Struct 1999;32(3):196–202.
[16] Rombach GA. Dry joint behavior of hollow box girder segmental bridge. Fib symposium: segmental construction in concrete, vol. 11, New Delhi; 2004. p. 26–9.